Monograph:
Tokhi, M.O. and Azad, A.K.M. (1995) Dynamic Simulation of Flexible Manipulator Systems with Structural Damping. Research Report. ACSE Research Report 595 . Department of Automatic Control and Systems Engineering

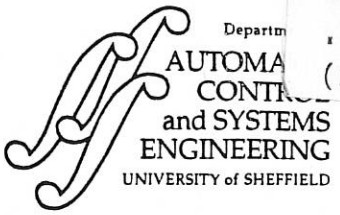

DYNAMIC SIMULATION OF FLEXIBLE MANIPULATOR SYSTEMS WITH STRUCTURAL DAMPING

M O Tokhi, H Poerwanto and A K M Azad

Department of Automatic Control and Systems Engineering,
The University of Sheffield, Mappin Street, Sheffield, S1 3JD, UK.

Tel: + 44 (0)114 2825136.
Fax: + 44 (0)114 2731 729.
E-mail: O.Tokhi@sheffield.ac.uk.

Research Report No. 595

August 1995

Abstract

This paper presents the development of a simulation environment characterising the dynamic behaviour of a flexible manipulator system incorporating hub inertia, payload and structural damping. A constrained planar single-link flexible manipulator is considered. A fourth-order partial differential equation model of the system, obtained through the utilisation of Lagrange equation and modal expansion method, including a mode frequency dependent damping term, is considered. A finite-dimensional discrete simulation of the flexible manipulator system is developed using a finite difference discretisation of the dynamic equation of motion of the manipulator. The algorithm thus developed is implemented on a digital processor and simulation results verifying the performance of the algorithm in characterising the dynamic behaviour of the manipulator under various loading conditions are presented and discussed.

Key words: *Discrete simulation, distributed parameter systems, finite difference method, flexible manipulators.*

CONTENTS

LIST OF TABLES AND FIGURES

1 Introduction

Flexible manipulator systems offer several advantages in contrast to the traditional rigid ones. These include faster system response, lower energy consumption, requiring relatively smaller actuators, reduced nonlinearity due to elimination of gearing, less overall mass and, in general, less overall cost. However, due to the distributed nature of the governing equations describing system dynamics, the control of flexible manipulators has traditionally involved complex processes (Aubrun, 1980; Balas, 1978; Omatu and Seinfeld, 1986). Moreover, to compensate for flexure effects and thus yield robust control the design focuses primarily on noncolocated controllers (Cannon and Schmitz, 1984; Harishima and Ueshiba, 1986). It is important initially to recognise the flexible nature of the manipulator and construct a mathematical model for the system that accounts for the interactions with actuators and payload. Such a model can be constructed using partial differential equations. A commonly used approach for solving a partial differential equation (PDE) representing the dynamics of a manipulator, sometimes referred to as the separation of variables method, is to utilise a representation of the PDE, obtained through a simplification process, by a finite set of ordinary differential equations. Such a model, however, does not always represent the fine details of the system (Hughes, 1987). A method in which the flexible manipulator is modelled as a massless spring with a lumped mass at one end and lumped rotary inertia at the other end has previously been proposed (Oosting and Dickerson, 1988; Feliu et al., 1992). Unfortunately, the solution obtained through this method is also not accurate and suffers from similar problems as in the case of the separation of variables method. The finite element (FE) method has also been previously utilised to describe the flexible behaviour of manipulators (Usoro et al., 1984; Dado and Soni, 1986). The computational complexity and consequent software coding involved in the FE method is a major disadvantage of this technique. However, as the FE method allows irregularities in the structure and mixed boundary conditions to be handled, the technique is found suitable in applications involving irregular structures. In applications involving uniform structures, such as the manipulator system considered here, the finite difference (FD) method is found to be more appropriate. Previous simulation studies of flexible beam systems have

demonstrated the relative simplicity of the FD method (Kourmoulis, 1990). Dynamic simulation is important from a system design and evaluation viewpoint. It provides a characterisation of the system in the real sense as well as allows on-line evaluation of controller designs. An investigation into the dynamic simulation of a flexible manipulator system is thus presented in this paper using FD methods.

The FD method is used to obtain an efficient numerical method of solving the PDE by developing a finite-dimensional simulation of the flexible manipulator system through a discretisation, both, in time and space (distance) coordinates. The algorithm proposed here allows the inclusion of distributed actuator and sensor terms in the PDE and modification of boundary conditions. The development of such an algorithm for a system with no damping has previously been reported (Tokhi and Azad, 1995). However, not much work on simulation of flexible manipulators with damping has been done. This paper presents the development of a simulation environment characterising the behaviour of a single-link flexible manipulator incorporating mode frequency dependent damping. The algorithm thus developed is implemented digitally and simulation results verifying its performance in characterising the behaviour of the system under various loading conditions are presented and discussed. The simulated system is constructed to provide a suitable platform for subsequent implementation and verification of various controller designs.

2 The flexible manipulator system

A description of a single-link flexible manipulator system is shown in Figure 1, where **XOY** and **POQ** represent the stationary and moving coordinates respectively, $\tau(t)$ represents the applied torque at the hub by a drive motor, M_p is the payload mass and I_h is the hub inertia. E, I and ρ represent the Young modulus, second moment of inertia and mass density per unit length of the manipulator respectively. The gravity effects are neglected and the motion of the manipulator is confined to the **XOY** plane.

The flexible manipulator system can be modelled as a pinned-free flexible beam, incorporating an inertia at the hub and payload mass at the end-point. The model is

developed through the utilisation of Lagrange equation and modal expansion method (Hastings and Book, 1987; Korolov and Chen, 1989). For an angular displacement θ and an elastic deflection u, the total (net) displacement $y(x,t)$ of a point along the manipulator at a distance x from the hub can be described as a function of both the rigid body motion $\theta(t)$ and elastic deflection $u(x,t)$ measured from the line **OP**;

$$y(x,t) = x\theta(t) + u(x,t) \tag{1}$$

The dynamic equations of motion of the manipulator can be obtained using the Hamilton's extended principle (Meirovitch, 1967) with the associated kinetic, potential and dissipated energies of the system. Ignoring the effects of the rotary inertia and shear deformation, a fourth order PDE representing the manipulator motion can, thus, be obtained as (Azad, 1994)

$$EI \frac{\partial^4 u(x,t)}{\partial x^4} + \rho \frac{\partial^2 u(x,t)}{\partial t^2} = - \rho x \ddot{\theta} \tag{2}$$

To obtain the corresponding boundary conditions, the following must hold

- The displacement at the hub ($u(0,t)$) must be zero,
- The total forces at the hub must be the same with the applied torque,
- The shear force at the end-point must be equal to $M_P \frac{\partial^2 u(x,t)}{\partial t^2}$ (Tse, et.al, 1980).
- The stress at the end-point must be zero, that is, no force should be present at the free end;

$$\begin{aligned} u(0,t) &= 0 \\ I_h \frac{\partial^3 u(0,t)}{\partial t^2 \partial x} - EI \frac{\partial^2 u(0,t)}{\partial x^2} &= \tau(t) \\ M_p \frac{\partial^2 u(l,t)}{\partial t^2} - EI \frac{\partial^3 u(l,t)}{\partial x^3} &= 0 \\ EI \frac{\partial^2 u(l,t)}{\partial x^2} &= 0 \end{aligned} \tag{3}$$

where l is the length of the manipulator. Equation (2) with the corresponding boundary conditions in equation (3) represents the dynamic equation of motion of the flexible

manipulator system assuming no damping in the system. In practice, however, such an effect is always present in the system.

There are several possible forms of damping within the system. These can be classified into three groups, depending on the source: (a) The manipulator itself has structural damping due to dissipation of energy within the manipulator material, (b) Viscous damping and Coulomb damping (stiction/friction) associated with driving motor, (c) External effects such as primarily air resistance as the manipulator rotates.

To incorporate damping in the governing dynamic equation of the system, a mode frequency dependent damping term proportional to $\frac{\partial^3 u(x,t)}{\partial x^2 \partial t}$ can be introduced (Davis and Hirschorn, 1988). Equation (2) can thus be modified to yield

$$EI \frac{\partial^4 u(x,t)}{\partial x^4} + \rho \frac{\partial^2 u(x,t)}{\partial t^2} - D_S \frac{\partial^3 u(x,t)}{\partial x^2 \partial t} = - \rho x \ddot{\theta} \qquad (4)$$

where D_S is the resistance to strain velocity, that is, rate of change of strain and $D_S \frac{\partial^3 u(x,t)}{\partial x^2 \partial t}$ represents the resulting damping moment dissipated in the manipulator structure during its dynamic operation. The corresponding boundary conditions can, thus, be written as

$$\begin{aligned} u(0,t) &= 0 \\ I_h \frac{\partial^3 u(0,t)}{\partial t^2 \partial x} - EI \frac{\partial^2 u(0,t)}{\partial x^2} &= \tau(t) \\ M_p \frac{\partial^2 u(l,t)}{\partial t^2} - EI \frac{\partial^3 u(l,t)}{\partial x^3} &= 0 \\ EI \frac{\partial^2 u(l,t)}{\partial x^2} &= 0 \end{aligned} \qquad (5)$$

Note in Figure 1 that as line **OP** is tangential to the manipulator at the hub, point **O** , the following holds

$$\frac{\partial u(0,t)}{\partial x} = 0 \qquad (6)$$

Thus, using equations (1) and (6) yield

$$\frac{\partial y(0,t)}{\partial x} = \theta(t)$$

Substituting for $u(x,t)$ from equation (1) into equations (4) and (5), manipulating and simplifying yields the governing equation of motion of the manipulator in terms of $y(x,t)$ as

$$EI \frac{\partial^4 y(x,t)}{\partial x^4} + \rho \frac{\partial^2 y(x,t)}{\partial t^2} - D_s \frac{\partial^3 y(x,t)}{\partial x^2 \partial t} = \tau(t) \tag{7}$$

with the corresponding boundary conditions as

$$\begin{aligned} y(0,t) &= 0 \\ I_h \frac{\partial^3 y(0,t)}{\partial x \partial t^2} - EI \frac{\partial^2 y(0,t)}{\partial x^2} &= \tau(t) \\ M_p \frac{\partial^2 y(l,t)}{\partial t^2} - EI \frac{\partial^3 y(l,t)}{\partial x^3} &= 0 \\ EI \frac{\partial^2 y(l,t)}{\partial x^2} &= 0 \end{aligned} \tag{8}$$

and initial conditions as

$$y(x,0) = 0, \quad \frac{\partial y(x,0)}{\partial x} = 0 \tag{9}$$

Equation (7) gives the fourth-order PDE which represents the dynamic equation describing the motion of the flexible manipulator. To solve this equation and thus, develop a suitable simulation environment characterising the behaviour of the system, the FD method can be used. Thus, a set of equivalent difference equations defined by the central finite difference quotients of the FD method are obtained by discretising the PDE in equation (7) with its associated boundary and initial conditions in equations (8) and (9). The process involves dividing the manipulator into n sections each of length Δx and considering the deflection of each section at sample times Δt, see Figure 2. In this manner, a solution of the PDE is obtained by generating the central difference formulae for the partial derivative terms of the response $y(x,t)$ of the manipulator at points $x = i.\Delta x$, $t = j.\Delta t$ (Azad, 1994 ; Burden and Faires, 1989; Lapidus, 1982);

$$
\begin{aligned}
\frac{\partial^2 y(x,t)}{\partial t^2} &= \frac{y_{i,j+1} - 2y_{i,j} + y_{i,j-1}}{\Delta t^2} \\
\frac{\partial^2 y(x,t)}{\partial x^2} &= \frac{y_{i+1,j} - 2y_{i,j} + y_{i-1,j}}{\Delta x^2} \\
\frac{\partial^3 y(x,t)}{\partial x^3} &= \frac{y_{i+2,j} - 2y_{i+1,j} + 2y_{i-1,j} - y_{i-2,j}}{2\Delta x^3} \\
\frac{\partial^4 y(x,t)}{\partial x^4} &= \frac{y_{i+2,j} - 4y_{i+1,j} + 6y_{i,j} - 4y_{i-1,j} + y_{i-2,j}}{\Delta x^4} \\
\frac{\partial^3 y(x,t)}{\partial t^2 \partial x} &= \frac{y_{i,j+1} - 2y_{i,j} + y_{i,j-1} - y_{i-1,j+1} + 2y_{i-1,j} - y_{i-1,j-1}}{\Delta x \Delta t^2} \\
\frac{\partial^3 y(x,t)}{\partial x^2 \partial t} &= \frac{y_{i+1,j} - 2y_{i,j} + y_{i-1,j} - y_{i+1,j-1} + 2y_{i,j-1} - y_{n-1,j-1}}{\Delta t \Delta x^2}
\end{aligned}
\tag{10}
$$

where, $y_{i,j}$ represents the response $y(x,t)$ at $x = i\Delta x$ and $t = j\Delta t$ or $y(x_i, t_j)$. Note that, a time-space discretisation is adopted in the evaluation of the response of the manipulator.

3 Development of the simulation algorithm

A solution of the PDE in equation (7) can be obtained by substituting for $\frac{\partial^2 y}{\partial t^2}$, $\frac{\partial^4 y}{\partial x^4}$ and $\frac{\partial^3 y}{\partial x^2 \partial t}$ from equation (10) and simplifying to yield

$$
\begin{aligned}
&\frac{EI}{\Delta x^4}\left[y_{i+2,j} - 4y_{i+1,j} + 6y_{i,j} - 4y_{i-1,j} + y_{i-2,j}\right] + \frac{\rho}{\Delta t^2}\left[y_{i,j+1} - 2y_{i,j} + y_{i,j-1}\right] \\
&\quad - \frac{D_S}{\Delta x^2 \Delta t}\left[y_{i+1,j} - 2y_{i,j} + y_{i-1,j} - y_{i+1,j-1} + 2y_{i,j-1} - y_{i-1,j-1}\right] = \tau(i,j)
\end{aligned}
$$

or

$$
\begin{aligned}
y_{i,j+1} = \frac{\Delta t^2}{\rho}\tau(i,j) &- c\left[y_{i+2,j} + y_{i-2,j}\right] + b\left[y_{i+1,j} + y_{i-1,j}\right] + a\,y_{i,j} - y_{i,j-1} \\
&+ d\left[y_{i+1,j} - 2\,y_{i,j} + y_{i-1,j} - y_{i+1,j-1} + 2\,y_{i,j-1} - y_{i-1,j-1}\right]
\end{aligned}
\tag{11}
$$

where $a = 2 - \frac{6EI\Delta t^2}{\rho \Delta x^4}$; $b = \frac{4EI\Delta t^2}{\rho \Delta x^4}$; $c = \frac{EI\Delta t^2}{\rho \Delta x^4}$; $d = \frac{D_S \Delta t}{\rho \Delta x^2}$.

Equation (11) gives the displacement of section $i+1$ of the manipulator at time step $j+1$. It follows from this equation that, to obtain the displacements $y_{n-1,j+1}$ and $y_{n,j+1}$, the displacements of the fictitious points $y_{n+2,j}$, $y_{n+1,j}$ and $y_{n+1,j-1}$ are required. These can be obtained using the boundary conditions related to the dynamic equation of the flexible

manipulator. The discrete form of the corresponding boundary conditions, obtained in similar manner as above, are

$$y_{0,j} = 0 \tag{12}$$

$$y_{-1,j} = y_{1,j} + \frac{\Delta x I_h}{EI\Delta t^2}\left[y_{1,j+1} - 2y_{1,j} + y_{1,j-1}\right] + \frac{\Delta t^2}{EI}\tau(j) \tag{13}$$

$$y_{n+2,j} = 2y_{n+1,j} - 2y_{n-1,j} + y_{n-2,j} + \frac{2\Delta x^3 M_p}{\Delta t^2 EI}\left[y_{n,j+1} - 2y_{n,j} + y_{n,j-1}\right] \tag{14}$$

$$y_{n+1,j} = 2y_{n,j} - y_{n-1,j} \tag{15}$$

In the following sections two cases, namely, the system with hub inertia and payload and the system without hub inertia and payload, are considered and investigated.

3.1 The hub displacement

Note that the torque is applied at the hub of the flexible manipulator. Thus, $\tau(i,j) = 0$ for $i \geq 1$. Using equations (11) and (12), the displacement $y_{1,j+1}$ can be obtained as

$$y_{1,j+1} = -c\left[y_{3,j} + y_{-1,j}\right] + b\,y_{2,j} + a y_{1,j} - y_{1,j-1} + d\left[y_{2,j} - 2y_{1,j} - y_{2,j-1} + 2y_{1,j-1}\right] \tag{16}$$

Substituting for $y_{-1,j}$ from equation (13) into equation (16) and simplifying yields

$$y_{1,j+1} = K_1 y_{1,j} + K_2 y_{2,j} + K_3 y_{3,j} + K_4 y_{1,j-1} + K_5 y_{2,j-1} + K_6 \tau(j) \tag{17}$$

where

$$K_1 = \frac{c\Delta t^2 EI + 2c\Delta x I_h + (a-2d)\Delta t^2 EI}{\Delta t^2 EI + c\Delta x I_h} \qquad K_4 = -\frac{c\Delta x I_h + (1-2d)\Delta t^2 EI}{\Delta t^2 EI + c\Delta x I_h}$$

$$K_2 = \frac{(b+d)\Delta t^2 EI}{\Delta t^2 EI + c\Delta x I_h} \qquad K_5 = -\frac{d\Delta t^2 EI}{\Delta t^2 EI + c\Delta x I_h}$$

$$K_3 = -\frac{c\Delta t^2 EI}{\Delta t^2 EI + c\Delta x I_h} \qquad K_6 = \frac{c\Delta x^2 \Delta t^2}{\Delta t^2 EI + c\Delta x I_h}$$

3.2 *The end-point displacement*

Using equation (11) for $i = n-1$, yields the displacement $y_{n-1,j-1}$ as

$$y_{n-1,j+1} = -c\left[y_{n-3,j} + y_{n+1,j}\right] + b\left[y_{n,j} + y_{n-2,j}\right] + a\,y_{n-1,j} - y_{n-1,j-1} + d\left[y_{n,j} - 2y_{n-1,j} + y_{n-2,j} - y_{n,j-1} + 2y_{n-1,j-1} - y_{n-2,j-1}\right] \quad (18)$$

Similarly, using equation (11) for $i = n$, yields the displacement $y_{n,j+1}$ as

$$y_{n,j+1} = -c\left[y_{n-2,j} + y_{n+2,j}\right] + b\left[y_{n+1,j} + y_{n-1,j}\right] + a\,y_{n,j} - y_{n,j-1} + d\left[y_{n+1,j} - 2y_{n,j} + y_{n-1,j} - y_{n+1,j-1} + 2y_{n,j-1} - y_{n-1,j-1}\right] \quad (19)$$

The fictitious displacements $y_{n+1,j}$ and $y_{n+2,j}$, appearing in equations (18) and (19), can be obtained using the boundary conditions in equations (14) and (15). $y_{n+1,j-1}$ can easily be obtained by shifting $y_{n+1,j}$ from time step j to time step $j-1$. Substituting for $y_{n+1,j}$ from equation (15) into equation (18) yields the displacement $y_{n-1,j+1}$ as

$$y_{n-1,j+1} = K_7\,y_{n-3,j} + K_8\,y_{n-2,j} + K_9\,y_{n-1,j} + K_{10}\,y_{n,j} + K_{11}\,y_{n-2,j-1} + K_{12}\,y_{n-1,j-1} + K_{13}\,y_{n,j-1} \quad (20)$$

where

$$K_7 = -c \qquad K_{11} = -d$$
$$K_8 = (b+d) \qquad K_{12} = -(1-2d)$$
$$K_9 = (a+c-2d) \qquad K_{13} = -d$$
$$K_{10} = -(2c-b-d)$$

Similarly, substituting for $y_{n+2,j}$ and $y_{n+1,j}$ from equations (14) and (15) into equation (19), and simplifying yields the displacement $y_{n,j+1}$ as

$$y_{n,j+1} = K_{14}\,y_{n-2,j} + K_{15}\,y_{n-1,j} + K_{16}\,y_{n,j} + K_{17}\,y_{n,j-1} \quad (21)$$

where

$$K_{14} = \frac{-2c\Delta t^2 EI}{\Delta t^2 EI + 2c\Delta x^3 M_P}$$

$$K_{15} = \frac{4c\Delta t^2 EI}{\Delta t^2 EI + 2c\Delta x^3 M_P}$$

$$K_{16} = \frac{\Delta t^2 EI}{\Delta t^2 EI + 2c\Delta x^3 M_P}\left\{a + 2b - 4c + \frac{4c\Delta x^3 M_P}{\Delta t^2 EI}\right\}$$

$$K_{17} = \frac{-\Delta t^2 EI}{\Delta t^2 EI + 2c\Delta x^3 M_P}\left\{\frac{2c\Delta x^3 M_P}{\Delta t^2 EI} + 1\right\}$$

Equations (11), (17), (20) and (21) represent the dynamic equation of the manipulator for all the grid points (stations) at specified instants of time t in the presence of hub inertia and payload.

3.3 Matrix formulation

Using matrix notation, equations (11), (17), (20) and (21) can be written in a compact form as

$$\mathbf{Y}_{i,j+1} = \mathbf{A}\mathbf{Y}_{i,j} + \mathbf{B}\mathbf{Y}_{i,j-1} + \mathbf{C}\mathbf{F}$$

where $\mathbf{Y}_{i,j+1}$ is the displacement of grid points $i = 1,2,\cdots,n$ of the manipulator at time step $j+1$, $\mathbf{Y}_{i,j}$ and $\mathbf{Y}_{i,j-1}$ are the corresponding displacements at time step j and $j-1$ respectively. **A** and **B** are constant $n \times n$ matrices whose entries depend on the flexible manipulator specification and the number of sections the manipulator is divided into, **C** is a constant matrix related to the given input torque and **F** is an $n \times 1$ matrix related to the time step Δt and mass per unit length of the flexible manipulator;

$$\mathbf{Y}_{i,j+1} = \begin{bmatrix} y_{1,j+1} \\ y_{2,j+1} \\ \vdots \\ y_{n,j+1} \end{bmatrix}, \quad \mathbf{Y}_{i,j} = \begin{bmatrix} y_{1,j} \\ y_{2,j} \\ \vdots \\ y_{n,j} \end{bmatrix}, \quad \mathbf{Y}_{i,j-1} = \begin{bmatrix} y_{1,j-1} \\ y_{2,j-1} \\ \vdots \\ y_{n,j-1} \end{bmatrix}$$

$$\mathbf{A} = \begin{bmatrix} K_1 & K_2 & K_3 & 0 & 0 & \cdots & 0 & 0 \\ (b+d) & (a-2d) & (b+d) & -c & 0 & \cdots & 0 & 0 \\ -c & (b+d) & (a-2d) & (b+d) & -c & \cdots & 0 & 0 \\ \vdots & \ddots & \ddots & \ddots & \ddots & \ddots & \ddots & \vdots \\ 0 & 0 & \cdots & -c & b+d & a-2d & b+d & -c \\ 0 & 0 & \cdots & 0 & K_7 & K_8 & K_9 & K_{10} \\ 0 & 0 & \cdots & 0 & 0 & K_{14} & K_{15} & K_{16} \end{bmatrix}$$

$$\mathbf{B} = \begin{bmatrix} K_4 & K_5 & 0 & 0 & 0 & \cdots & 0 & 0 \\ -d & 2d-1 & -d & 0 & 0 & \cdots & 0 & 0 \\ 0 & -d & 2d-1 & -d & 0 & \cdots & 0 & 0 \\ \vdots & \ddots & \ddots & \ddots & \ddots & \ddots & \ddots & \vdots \\ 0 & 0 & \cdots & 0 & -d & 2d-1 & -d & 0 \\ 0 & 0 & \cdots & 0 & 0 & K_{11} & K_{12} & K_{13} \\ 0 & 0 & \cdots & 0 & 0 & 0 & 0 & K_{17} \end{bmatrix}$$

$$\mathbf{C} = \tau(j) \quad , \mathbf{F} = \begin{bmatrix} K_6 & 0 & \cdots & 0 \end{bmatrix}^T$$

3.4 The system without hub inertia and payload

In this section, the system is considered with no inertia in the hub and no payload at the end-point. This allows investigating the effect of hub inertia and payload on the characteristics of the manipulator. The boundary conditions for this situation are obtained using equation (8) by setting $I_h = 0$ and $M_P = 0$. Thus, using equations (17), (20) and (21) with equation (11) yield the corresponding element values of the matrices **A**, **B** and **F** for the system without hub inertia and payload as

$$\begin{aligned} K_1 &= c + (a-2d) & K_{10} &= (b-2c+d) \\ K_2 &= (b+d) & K_{11} &= -d \\ K_3 &= -c & K_{12} &= -(1-2d) \\ K_4 &= -(1-2d) & K_{13} &= -d \\ K_5 &= -d & K_{14} &= -2c \\ K_6 &= c\Delta x^2/EI & K_{15} &= 4c \\ K_7 &= -c & K_{16} &= a+2b-4c \\ K_8 &= (b+d) & K_{17} &= -1 \\ K_9 &= (a+c-2d) \end{aligned}$$

4 Simulation environment set-up

To test and evaluate the performance of the simulation algorithm the following situations are considered:

(a) The system without hub inertia and payload,

(b) The system with hub inertia and no payload,

(c) The system with hub inertia and payload.

A bang-bang torque input with an amplitude of 0.1 Nm and duration of 0.6 seconds is used to excite the system. This is shown in Figure 3. The total simulation time is set to 1.2 seconds and the system behaviour at the hub and end-point observed and recorded.

The simulation environment was set up to characterise a motor-driven aluminum type single-link flexible manipulator of physical dimensions and characteristics given in Table 1. These correspond to a physically constructed flexible manipulator system [21]. For a reasonable level of accuracy to be achieved, the manipulator was divided into 19 equal-length sections within the FD discretisation process. To demonstrate the effect of damping, two typical values, namely, Ds = 0.024 and 0.148 are used. The time response as well as the corresponding spectral density of the system under each condition are recorded and presented to assess the effect of damping for various payloads. The damping, in the real system, is expected not to change the resonance mode of the system and to bring the residual movements (vibrations) to converge to zero as the energy is dissipated.

5 Simulation results

The set of results presented below show the performance of the simulation algorithm in characterising the flexible manipulator to the excitation in Figure 3 under three situations, namely, (a) $D_s = 0.0$, (b) $D_s = 0.024$ and (c) $D_s = 0.148$, over a duration of 1.2 seconds.

Figure 4 shows the time-domain representation and corresponding spectral density of end-point displacement for the system without hub inertia and payload. Figure 5 shows the corresponding time-domain representation and spectral density of the end-point residual

motion (vibrations) of the system. It is noted that with $D_s = 0.0$ the system response is persistently oscillatory and the oscillations converge to zero faster with increasing D_s. This is also evident in the corresponding spectral densities of the response, where the levels at the resonant modes decease with increasing D_s. The response in each case reaches the demanded level of 178.9 mm within similar time scales. The first three resonant modes, as noted, are found to be at 11.7 Hz, 41.6 Hz and 81.6 Hz respectively, which are reasonably close to those of the actual system. It is important to note that the resonant frequencies as well as the steady-state level of response of the system are not affected by the value of D_s.

Figure 6 shows the time-domain representation and corresponding spectral density of end-point displacement for the system with hub inertia and no payload. Figure 7 shows the corresponding time-domain representation and spectral density of the end-point residual motion of the system. A comparison of these with Figures 4 and 5 reveals that inclusion of hub inertia results in an increase in the level of vibrations at the resonant modes. Thus, the system response settling time increases. Moreover, the frequencies at the resonant modes decrease with the inclusion of hub inertia. As noted in Figures 6 and 7, the first three resonant modes are located at 11.6 Hz, 31.7 Hz and 61.7 Hz respectively. It is further noted that inclusion of the hub inertia has resulted in a drop in the steady-state level of system response from 178.9 mm (see Figure 4) to 176.4 mm.

To study the effect of payload on the characteristics of the system, the simulation algorithm was tested with a payload of 10 grams at the end-point. Figure 8 shows the time-domain representation and corresponding spectral density of end-point displacement for the system with hub inertia and the 10 grams payload. Figure 9 shows the corresponding time-domain representation and spectral density of the end-point residual motion of the system. A comparison of these with the results in Figures 4 to 7 reveals that the level of vibrations at the resonant modes decrease with the inclusion of a payload. Moreover, the steady-state level of response of the system has deceased with the inclusion of the payload. Furthermore, it is noted that the frequencies at the resonant modes have decreased. This effect is seen to be more pronounced at the higher modes. To illustrate the effect of hub inertia and payload on the characteristics of the system quantitatively, the results obtained

from Figures 4 to 9 are summarised in Table 2. It is seen that inclusion of hub inertia and payload both result in a decrease in the frequencies of the resonant modes and a reduction in the steady-state level of system response. The level of vibrations at the resonant modes, on the other hand, increase with the hub inertia but decease with a payload. These effects are further evidenced consistently in Figures 10, 11 and 12 which show the response of the system as monitored at the hub for the three situations considered above.

Incorporating a payload at the end-point, as noted in Figures 8, 9 and 12, affects the characteristics of a flexible manipulator. This includes the frequencies of the resonant modes, steady-state level of response of the system and level of vibrations at the resonant modes. The extent of these effects will vary with the amount of payload. To investigate this, the algorithm was set up with various amounts of payload and the effect on the response of the system was monitored. Figures 13 and 14 show the time-domain representation and the corresponding spectral densities of end-point displacement, respectively, for various payloads with $D_s = 0.024$. It is noted that the steady-state level of response of the system as well as the frequencies of the resonant modes decease with increasing payloads. A similar trend is observed with the level of vibrations at the second and higher resonant modes in relation to the payload. However, the effect on the level of vibrations at the first resonant mode does not appear to follow this general trend. These observations are important from a control viewpoint in a practical environment where a manipulator will usually be subjected to various amounts of payload.

6 Conclusion

A numerical method of solution of the governing PDE describing the characteristic behaviour of a flexible manipulator system incorporating the effects of hub inertia, payload and damping has been presented and discussed. A finite difference simulation algorithm characterising the behaviour of the system has initially been developed without hub inertia and payload. The simulation algorithm has then been extended to include the effect of hub inertia and payload.

Simulation results with and without the effects of the hub inertia show that the steady-state level of system response is slightly reduced with the hub inertia. The levels of vibration at the resonant modes of the system, on the other hand, have been found to increase with the hub inertia leading to a longer settling time in the system response. Moreover, the frequencies at the resonant modes of the system have been found to decrease with the inclusion of hub inertia.

It has been demonstrated that incorporating a payload at the end-point of the system results in a reduction in the steady-state level of response as well as in the resonant frequencies of the system. The level of vibrations at the resonant modes, however, vary with varying payloads; a decreasing trend at lower payloads and an increasing trend at higher payloads has been observed.

It has been demonstrated that incorporating a mode frequency dependent damping term within the governing dynamic equation of the flexible manipulator leads to a more realistic characterisation of the behaviour of the system. As expected, the damping term thus incorporated has been shown to have no effect on the resonant frequencies and steady-state level of response of the system. The oscillations in the system response, however, converge to zero with time; the settling time becoming shorter with increasing amounts of damping. The results of this investigation have shown that a reasonably accurate simulation environment characterising the behaviour of a flexible manipulator system for use as a test and verification platform of controller designs can be developed using finite difference discretisation methods.

7 References

AUBRUN, J.-N. (1980). Theory of the structures by low-authority controllers, *Journal of Guidance and Control*, **3**, pp. 441-451.

AZAD, A. K. M. (1994). *Analysis and design of control mechanisms for flexible manipulator systems*, PhD thesis, Department of Automatic Control and Systems Engineering, The University of Sheffield, UK.

BALAS, M. J. (1978). Feedback control of flexible systems, *IEEE Transaction on Automatic Control*, **AC-23**, pp. 673-679.

BURDEN, R. L. and FAIRES, J. D. (1989). *Numerical analysis*, PWS-KENT Publishing Company, Boston.

CANNON, R. H. and SCHMITZ, E. (1984). Initial experiments on the end-point control of a flexible one-link robot, *International Journal of Robotic Research*, **3**, pp. 62-75.

DADO, M. and SONI, A. H. (1986). A Generalized approach for forward and inverse dynamics of elastic manipulators, *Proceedings of IEEE Conference on Robotics and Automation*, San Francisco, pp. 359-364.

DAVIS, J. H. and HIRSCHORN, R. M. (1988). Tracking control of flexible robot link, *IEEE Transactions on Automatic Control*, **33**, pp. 238-248.

FELIU, V., RATTAN, K. S. and BROWN, H. B., Jr. (1992). Modelling and control of single link flexible arms with lumped masses, *Transaction of ASME Journal of Dynamic Systems, Measurement, and Control*, **114**, pp. 59-69.

HARISHIMA, F. and UESHIBA, T. (1986). Adaptive control of flexible arm using end-point position sensing, *Proceedings of Japan-USA Symposium of Flexible Automation*, 14-18 July, Osaka, pp. 225-229.

HASTINGS, G. G. and BOOK, W. J. (1987). A linear dynamic model for flexible robotic manipulator, *IEEE Control Systems Magazine*, **7**, pp. 61-64.

HUGHES, P. C. (1987). Space structure vibration modes: How many exists? Which are important, *IEEE Control Systems Magazine*, **7**, pp. 22-28.

KOROLOV, V. V. and CHEN, Y. H. (1989). Controller design robust to frequency variation in a one-link flexible robot arm, *Journal of Dynamic Systems, Measurement and Control*, **111**, pp. 9-14.

KOURMOULIS, P. K. (1990). *Parallel processing in the simulation and control of flexible beam structures*, PhD thesis, Department of Automatic Control and Systems Engineering, The University of Sheffield, UK.

LAPIDUS, L. (1982). *Numerical solution of partial differential equations in science and engineering*, John Wiley and Sons, New York.

MEIROVITCH, L. (1967). *Analytical methods in vibrations*, Macmillan, New York.

OMATU, S. and SEINFELD, J. H. (1986). Optimal sensor actuator locations for linear distributed parameter systems, *Proceedings of 4th IFAC Symposium on Control of Distributed Parameter Systems*, Los Angeles, pp. 215-220.

OOSTING, K. and DICKERSON, S. L. (1988). Simulation of a high-speed lightweight arm, *Proceedings of the IEEE International Conference on Robotics and Automation*, Philadelphia, pp. 494-496.

TOKHI, M. O. and AZAD, A. K. M. (1995). Real-time finite difference simulation of a single-link flexible manipulator system incorporating hub inertia and payload, *Proceedings of IMechE-I: Journal of Systems and Control Engineering*, **209**, (I1), pp. 21-33.

TOKHI, M. O. and AZAD, A. K. M. (1995). *Design anf development of a laboratory-scale single-link flexible manipulator system*, Reserach Report No. 594, Department of Automatic Control and Systems Engineering, The University of Sheffield, UK.

TSE, F.S., MORSE, I.E. and HINKLE, T.R. (1980). *Mechanical Vibrations Theory and Applications*, Allyn and Bacon Inc., Boston.

USORO, P. B., NADIRA, R. and MAHIL, S. S. (1984). A finite element/Lagrange approach to modelling lightweight flexible manipulator, *Transaction of ASME Journal of Dynamic Systems Measurement and Control*, **108**, pp. 198-205.

Table 1: Parameters and characteristics of the flexible manipulator system.

Parameter	Value
Length	960.0 mm
Width	19.008 mm
Thickness	3.2004 mm
Mass density per unit volume	2710 kg/m^3
Second moment of inertia, I	5.1924×10^{-11} m^4
Young modulus, E	71×10^{9} N/m^2
Moment of inertia, I_b	0.04862 kgm^2
Hub inertia, I_h	5.86×10^{-4} kgm^2
First flexible mode	12.137 Hz
Second flexible mode	36.132 Hz
Third flexible mode	88.86 Hz

Table 2: System response characteristics with hub inertia and payload.

			MODE 1		MODE 2		MODE 3	
Condition	D_s	D (mm)	F (Hz)	Res (mm)	F (Hz)	Res (mm)	F (Hz)	Res (mm)
Without hub	0.000	178.9	11.7	3.9×10^{-3}	41.6	2.5×10^{-4}	81.6	5.0×10^{-5}
inertia and	0.024	178.9	11.7	3.9×10^{-3}	41.6	1.8×10^{-4}	81.6	6.8×10^{-5}
payload	0.148	178.9	11.7	1.0×10^{-3}	41.6	3.0×10^{-5}	81.6	9.0×10^{-6}
With hub	0.000	176.4	11.6	10×10^{-3}	31.7	4.0×10^{-4}	61.7	3.9×10^{-4}
inertia and	0.024	176.4	11.6	6.5×10^{-3}	31.7	3.2×10^{-4}	61.7	6.0×10^{-5}
no payload	0.148	176.4	11.6	1.7×10^{-3}	31.7	1.3×10^{-4}	61.7	2.6×10^{-5}
With hub	0.000	148.6	11.6	3.8×10^{-3}	31.6	1.1×10^{-4}	58.3	3.0×10^{-4}
inertia and	0.024	148.6	11.6	2.6×10^{-3}	31.6	3.2×10^{-4}	58.3	2.0×10^{-5}
10g payload	0.148	148.6	11.6	8.0×10^{-4}	31.6	8.0×10^{-5}	58.3	1.6×10^{-5}

D_s : Damping constant.
D : End-point displacement.
F : Frequency of the resonance mode
Res : End-point residual movements (vibrations).

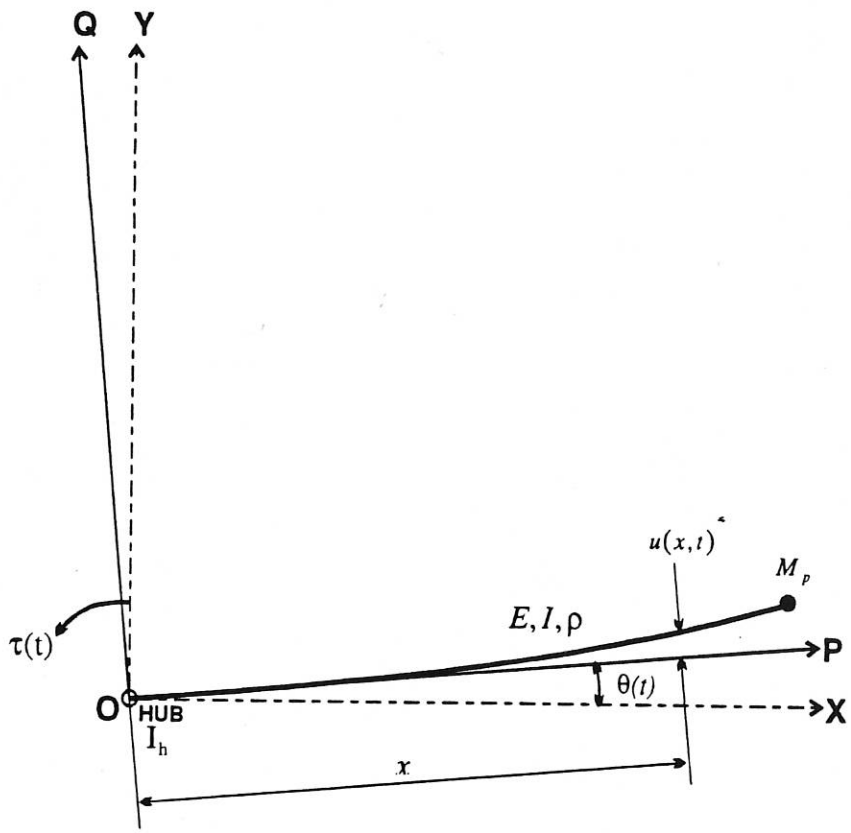

Figure 1: Description of the flexible manipulator system.

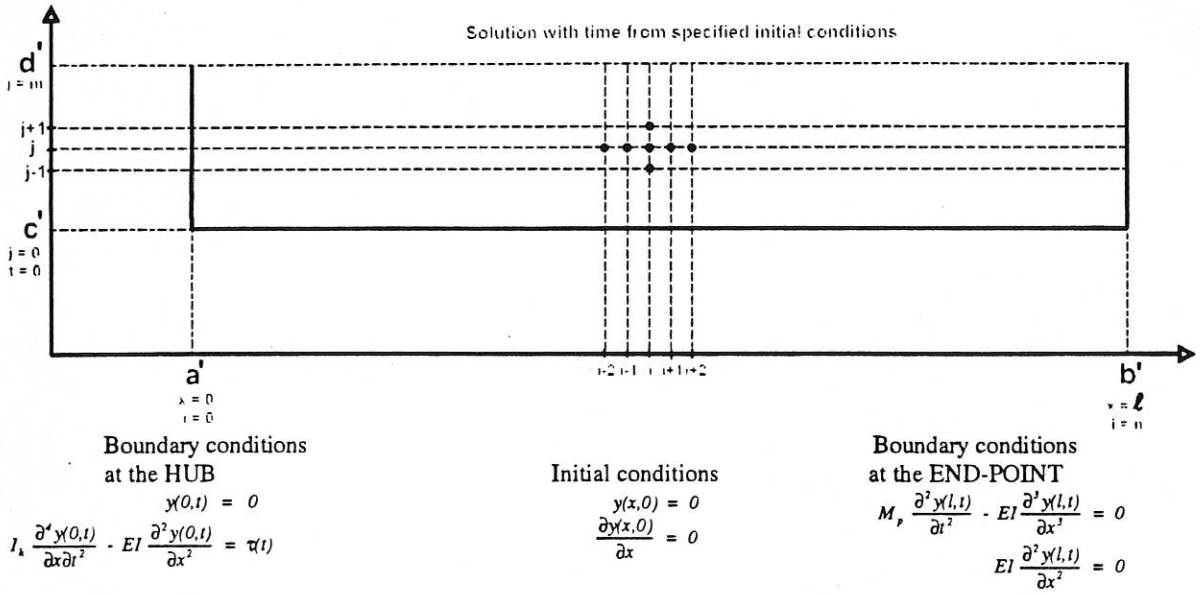

Figure 2: Finite difference discretisation in time and space variables.

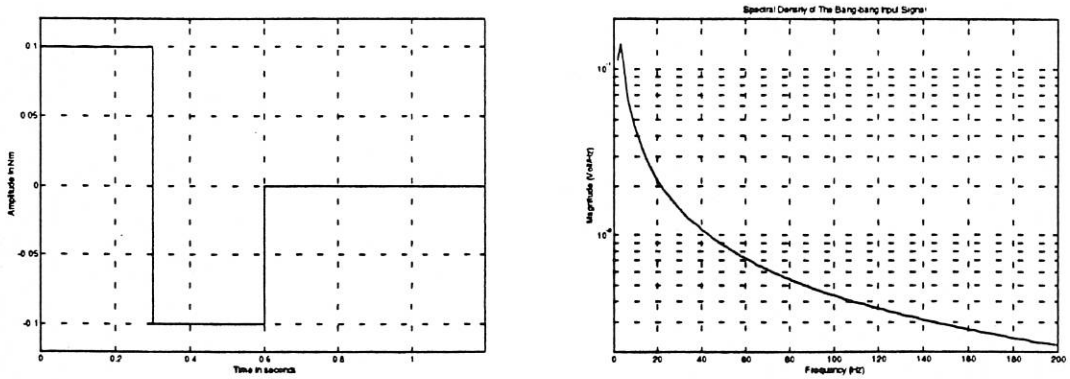

(a) (b)

Figure 3: Bang-bang input signal; (a) Time-domain. (b) Spectral density.

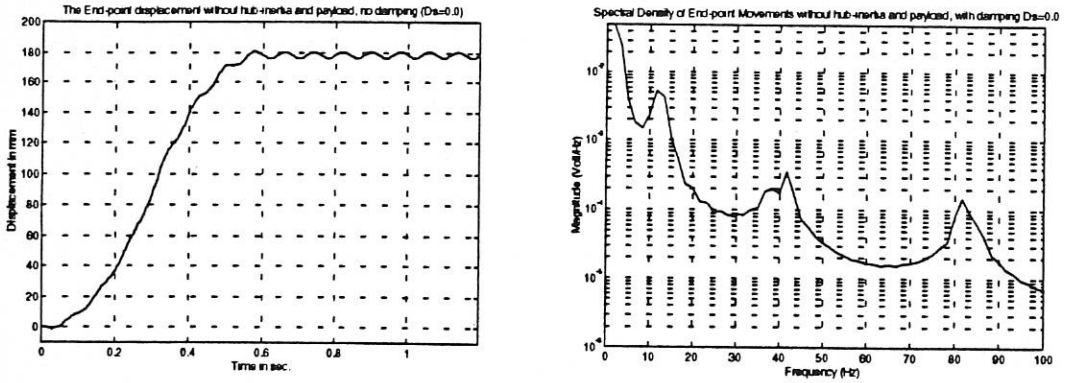

(a)

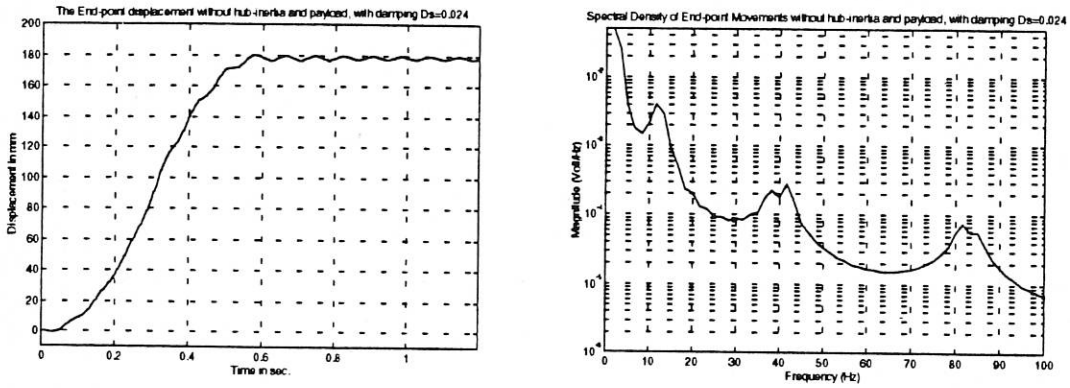

(b)

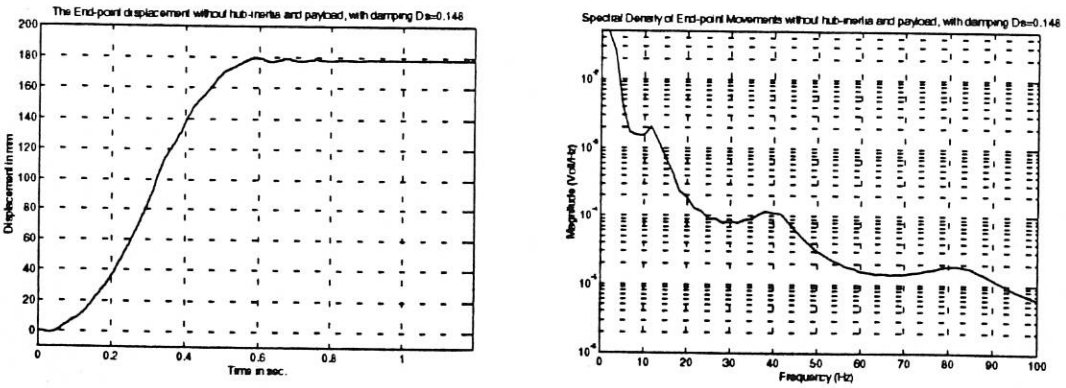

(c)

Figure 4: End-point movement of the flexible manipulator without hub-inertia and payload; (a) $D_s = 0.0$, (b) $D_s = 0.024$, (c) $D_s = 0.148$.

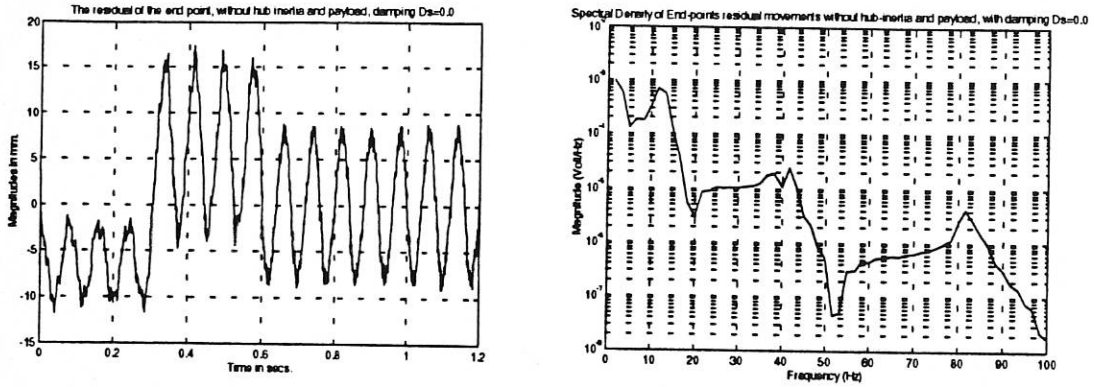

(a)

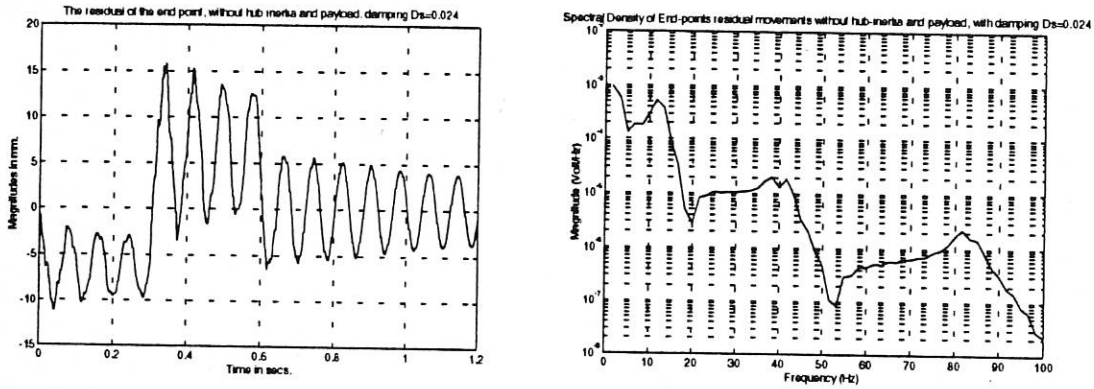

(b)

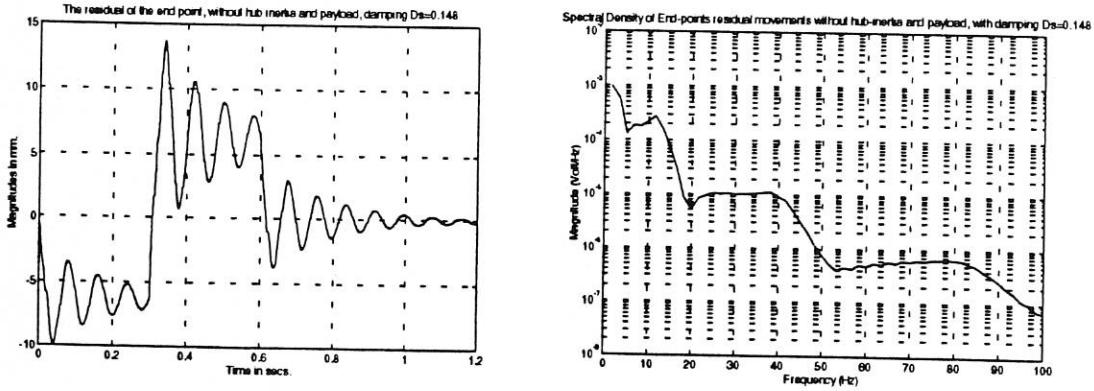

(c)

Figure 5: End-point residual motion of the flexible manipulator without hub inertia and payload; (a) $D_s = 0.0$, (b) $D_s = 0.024$, (c) $D_s = 0.148$.

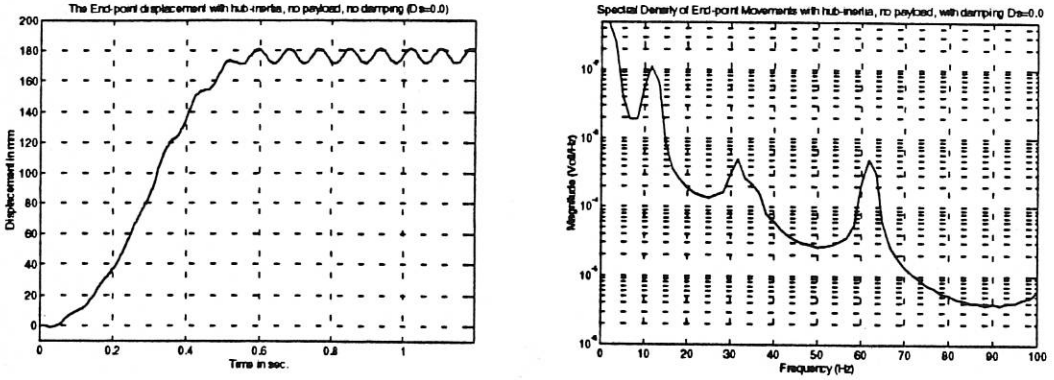

(a)

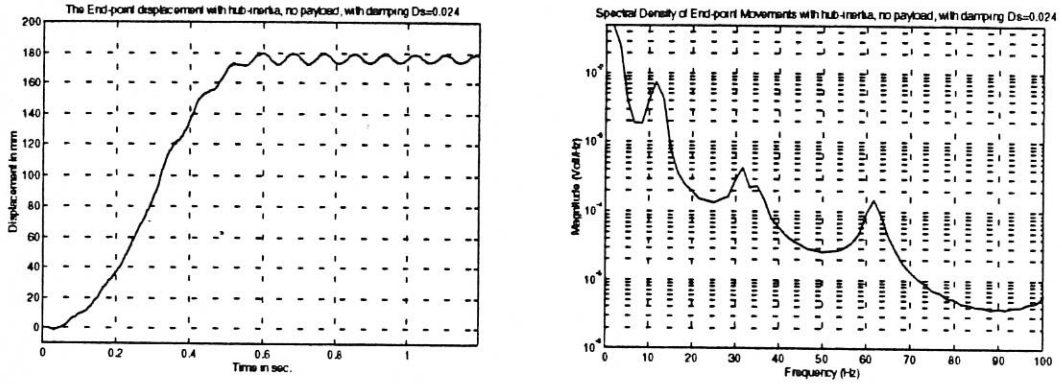

(b)

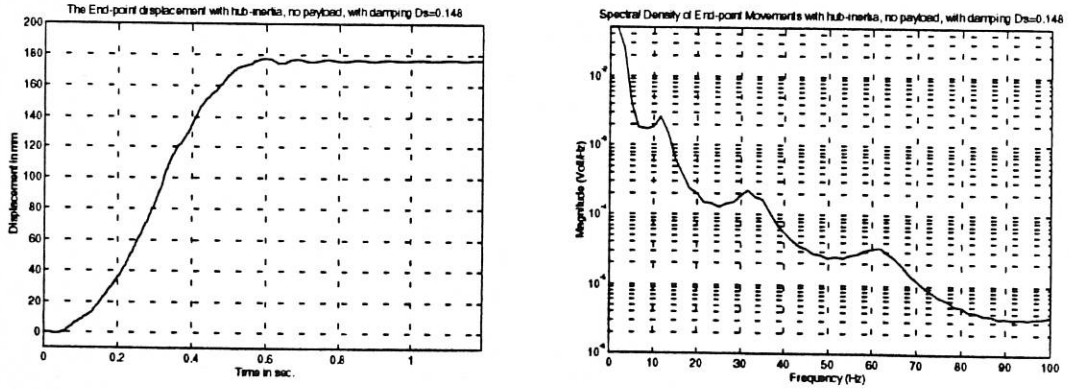

(c)

Figure 6: End-point movement of the flexible manipulator, with hub-inertia and no payload; (a) $D_s = 0.0$, (b) $D_s = 0.024$, (c) $D_s = 0.148$.

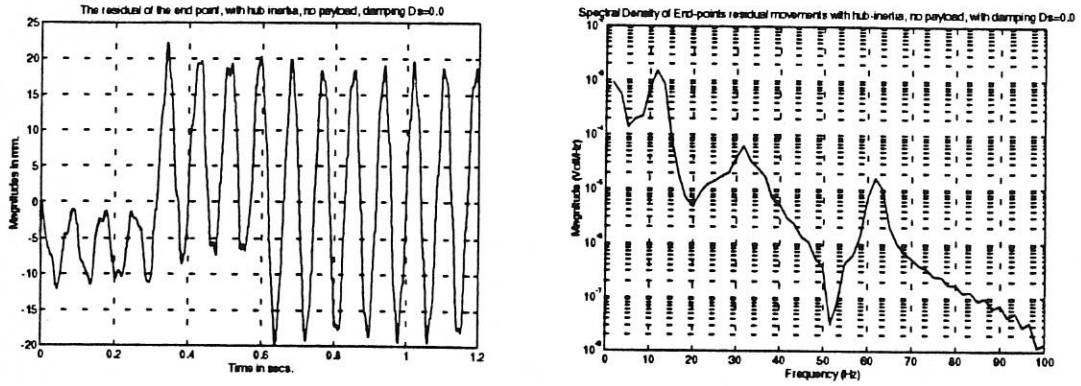

(a)

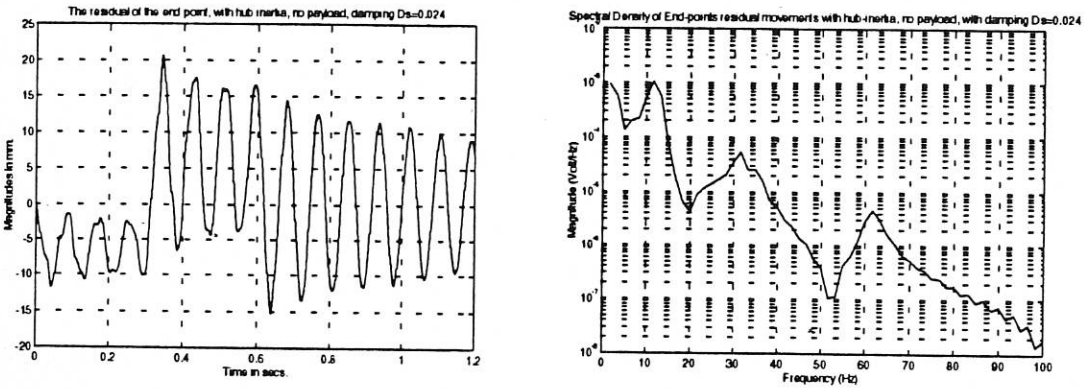

(b)

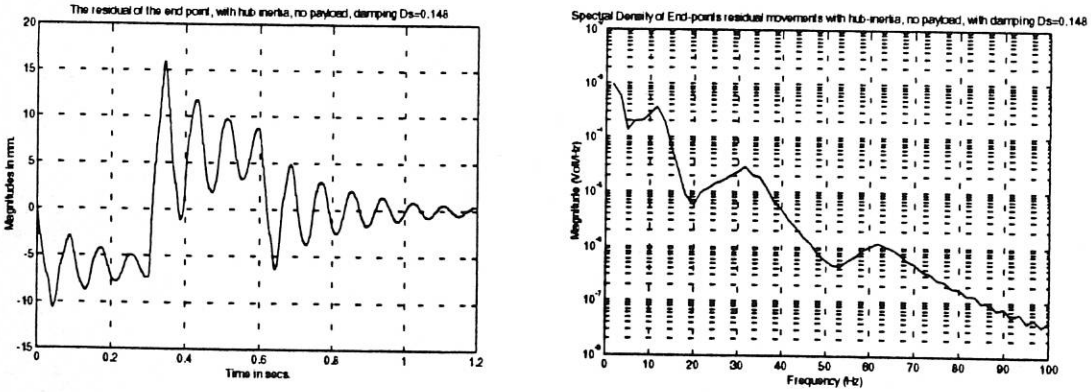

(c)

Figure 7: End-point residual motion of the flexible manipulator with hub inertia and no payload; (a) $D_s = 0.0$, (b) $D_s = 0.024$, (c) $D_s = 0.148$.

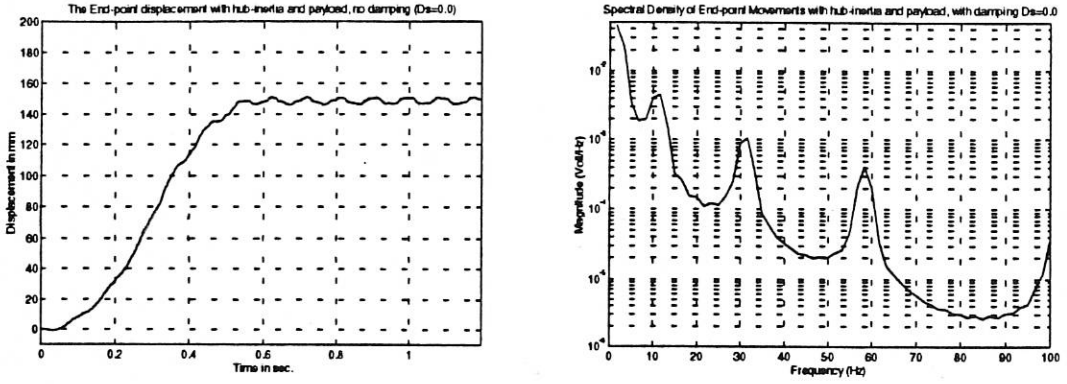

(a)

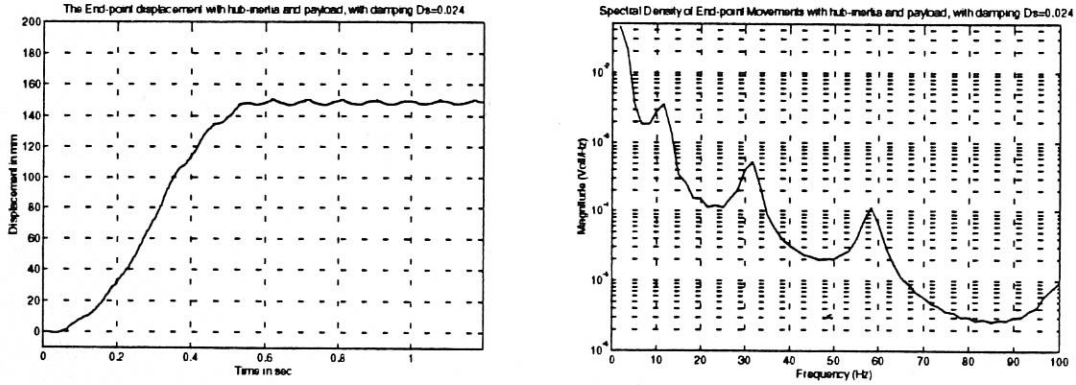

(b)

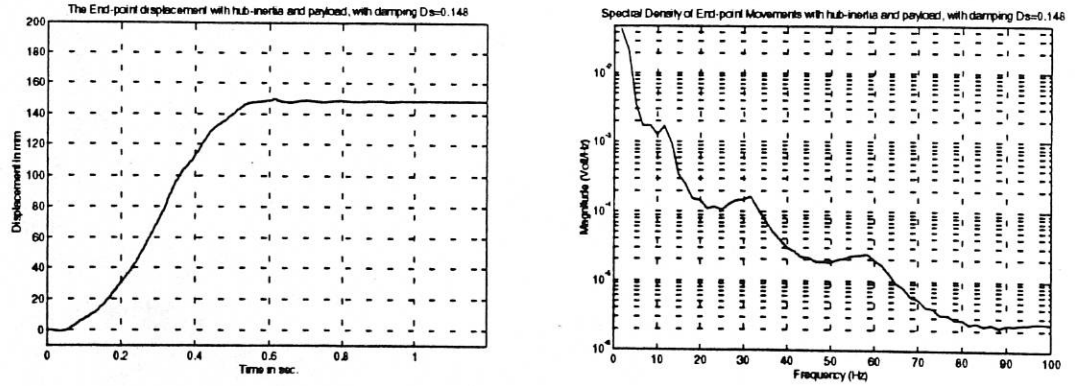

(c)

Figure 8: End-point movement of the flexible manipulator with hub-inertia and 10 grams payload; (a) $D_s = 0.0$, (b) $D_s = 0.024$, (c) $D_s = 0.148$.

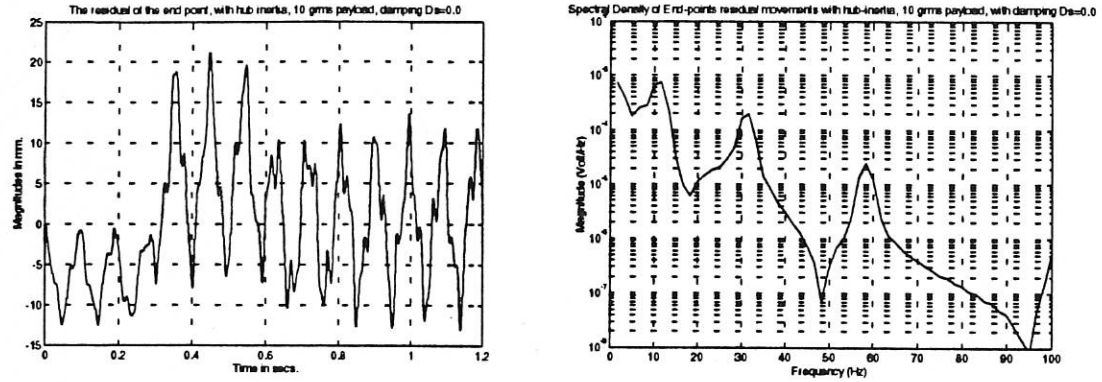

(a)

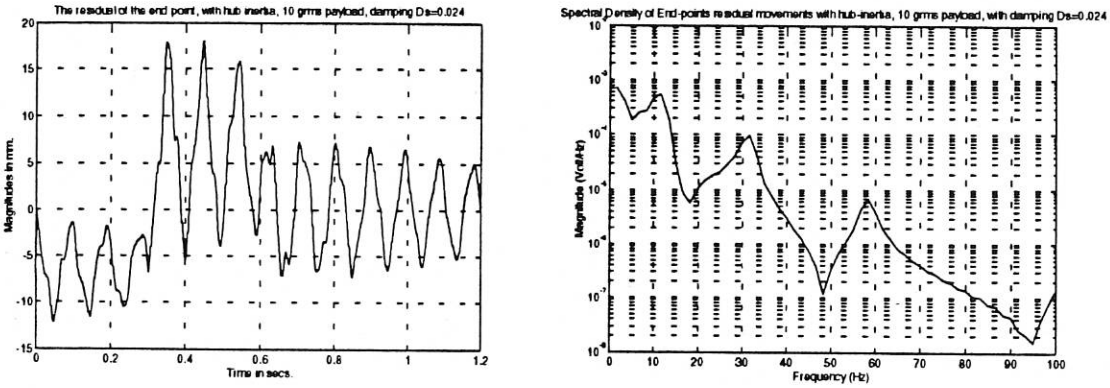

(b)

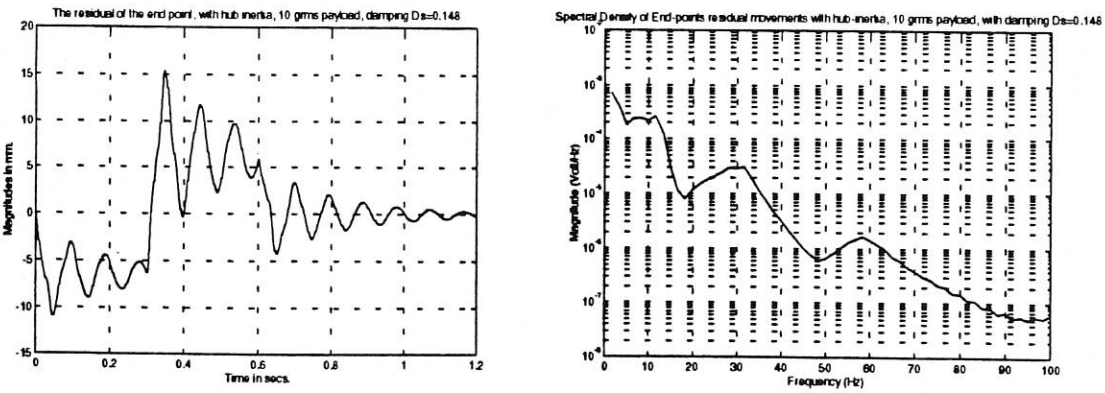

(c)

Figure 9: End-point residual motion of the flexible manipulator with hub inertia and 10 grams payload; (a) $D_s = 0.0$, (b) $D_s = 0.024$, (c) $D_s = 0.148$.

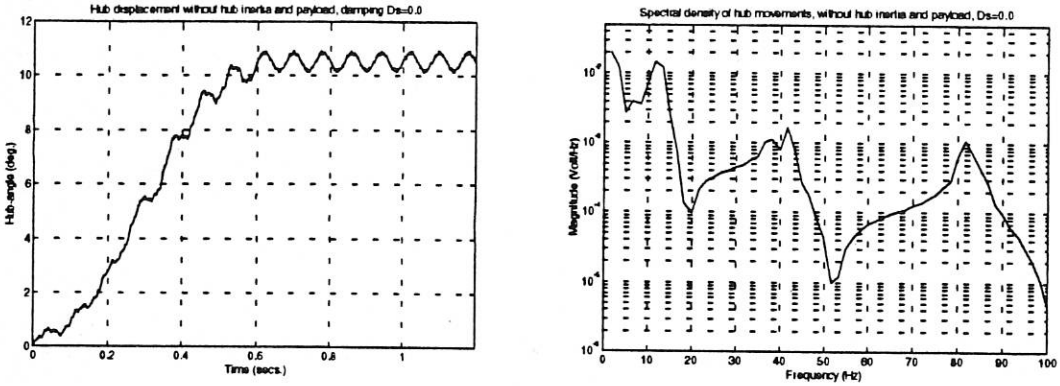

(a)

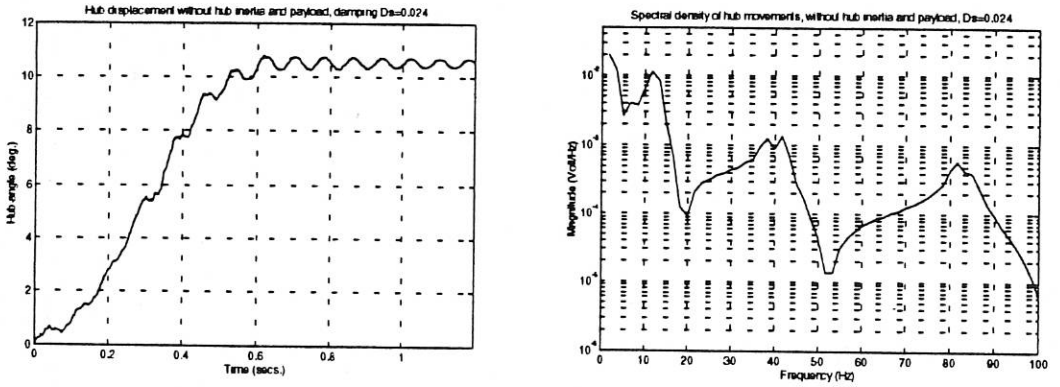

(b)

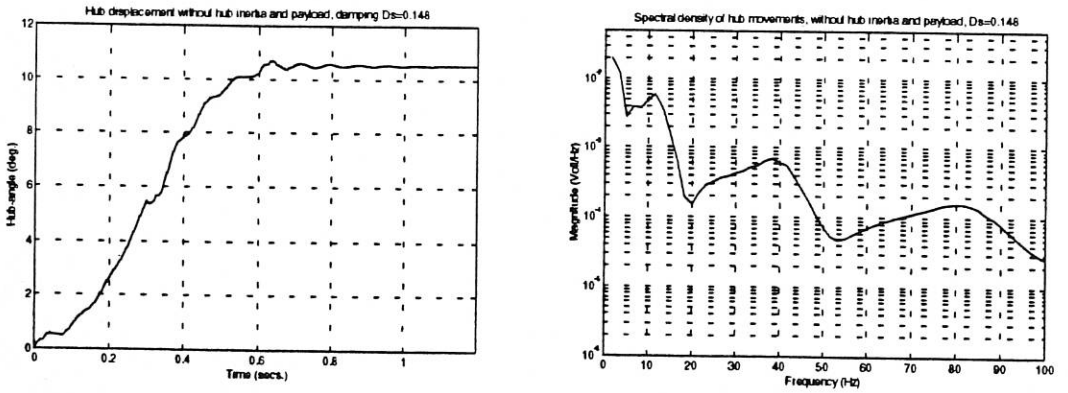

(c)

Figure 10: Hub angle displacement of the flexible manipulator without hub inertia and payload; (a) $D_s = 0.0$, (b) $D_s = 0.024$, (c) $D_s = 0.148$.

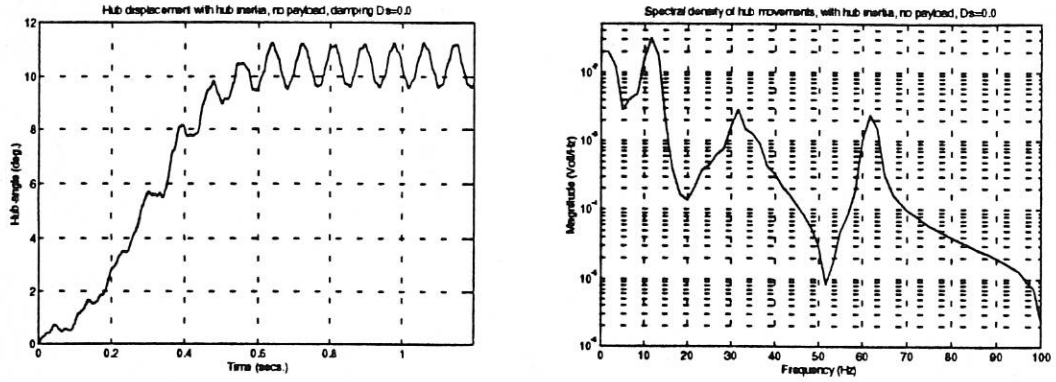

(a)

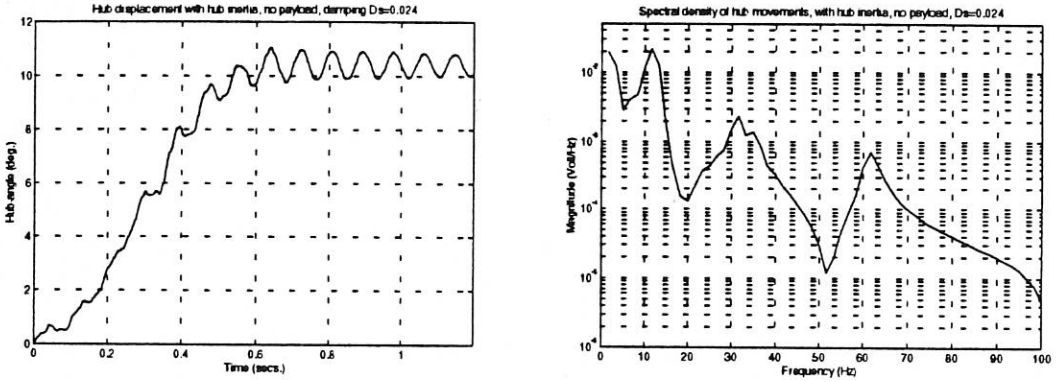

(b)

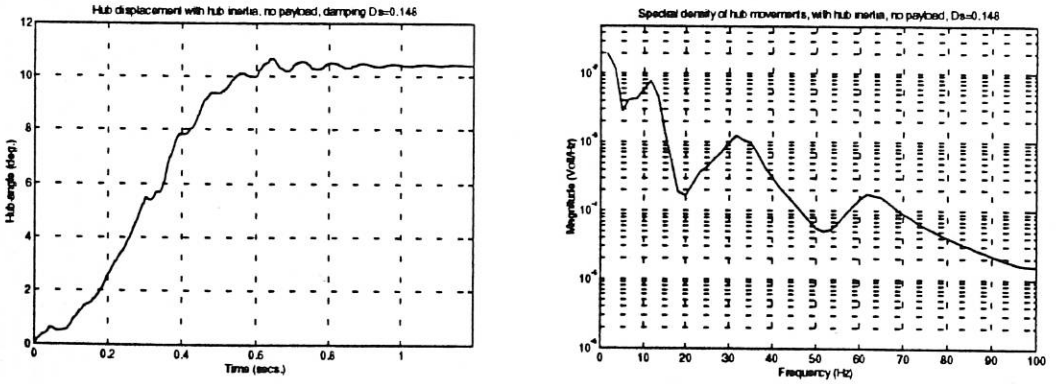

(c)

Figure 11: Hub angle displacement of the flexible manipulator with hub inertia and no payload; (a) $D_s = 0.0$, (b) $D_s = 0.024$, (c) $D_s = 0.148$.

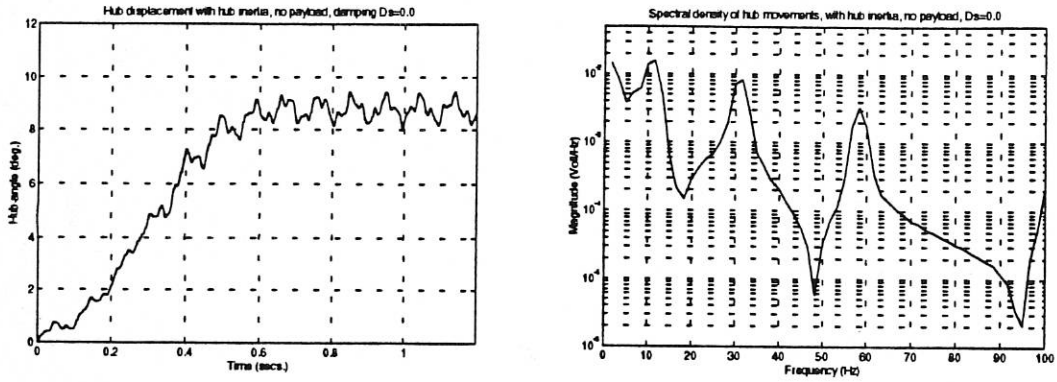

(a)

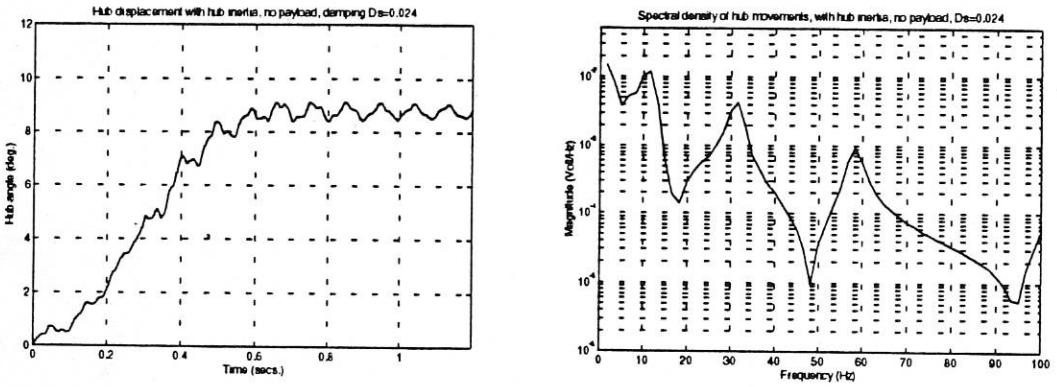

(b)

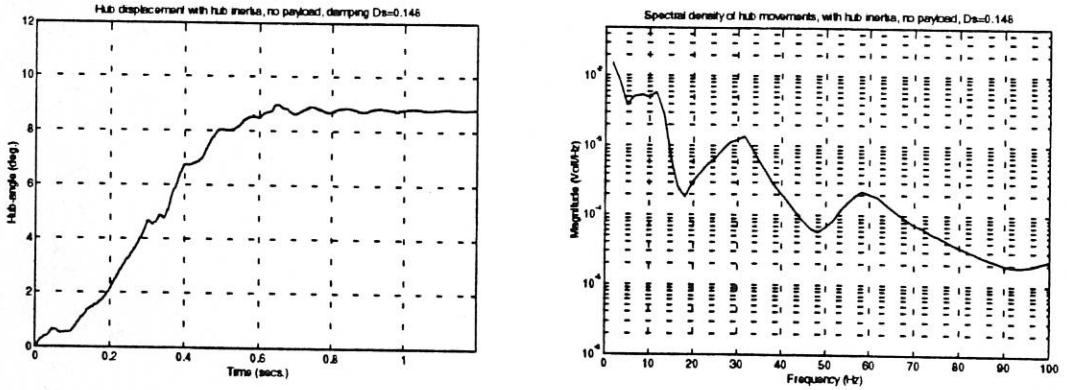

(c)

Figure 12: Hub angle displacement of the flexible manipulator with hub inertia and 10 grams payload; (a) $D_s = 0.0$, (b) $D_s = 0.024$, (c) $D_s = 0.148$.

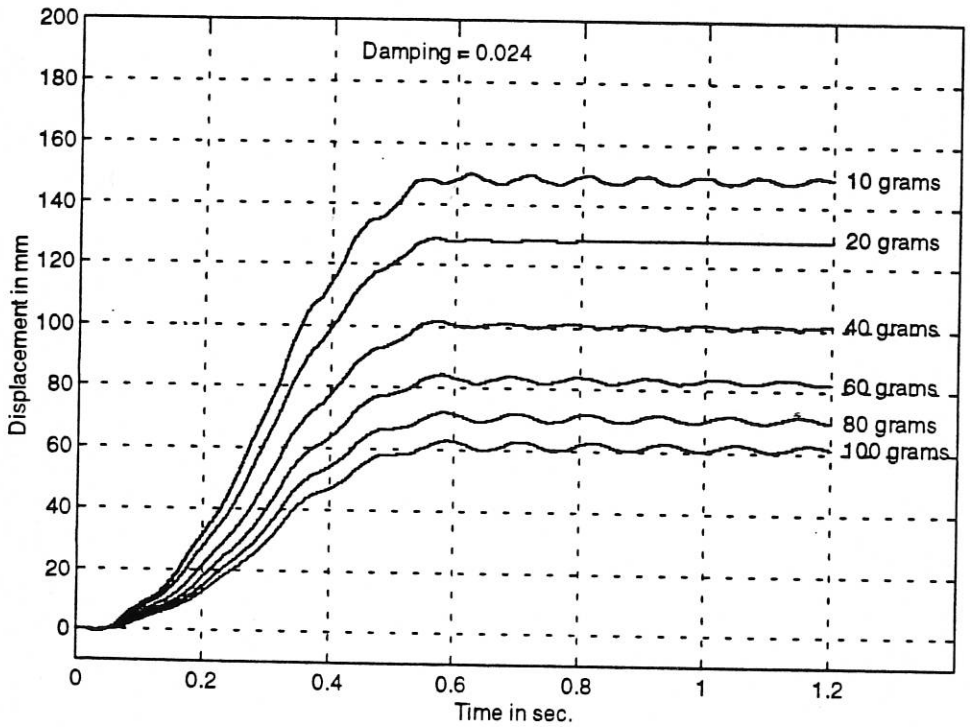

Figure 13: End-point movement of the flexible manipulator for various payloads.

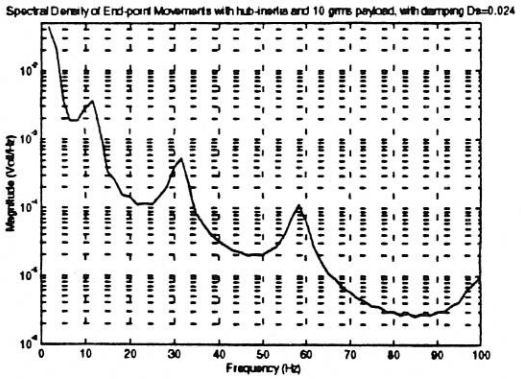

(a) 10 grms payload.

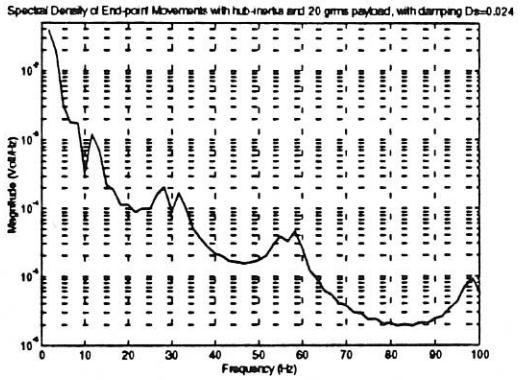

(b) 20 grms payload.

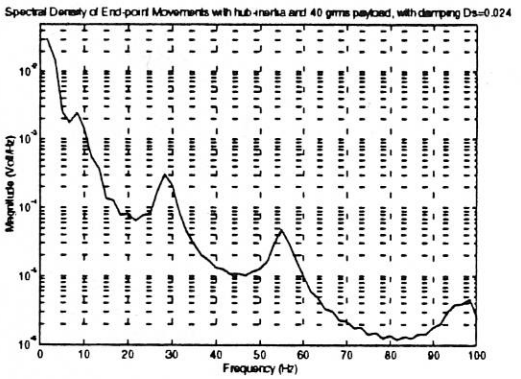

(c) 40 grms payload.

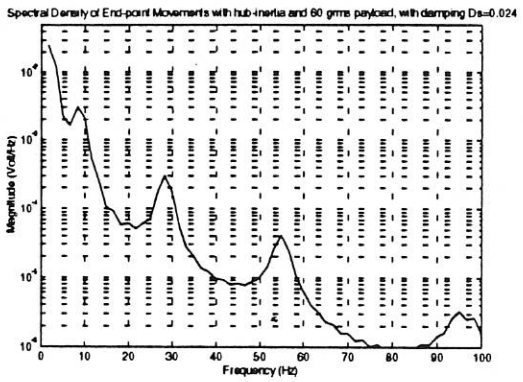

(d) 60 grms payload.

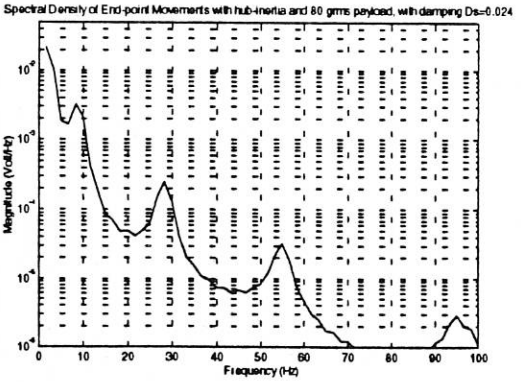

(e) 80 grms payload.

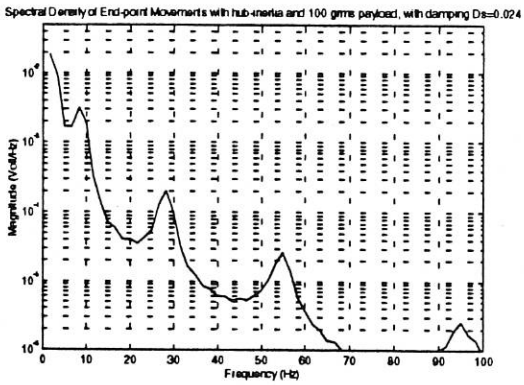

(f) 100 grms payload.

Figure 14: Spectral density of the end-point movement of the flexible manipulator for various payloads.